

Experiential Study on Corrosion in Amine Gas Treatment Plant

Abdalla.A.M.Ali*¹, Prof. Dr. Zulkefli Bin Yaacob², Prof. Dr. Abdurahman
Hamid Nour³

¹Department of Sciences and Technology, Higher Institute of Sciences and Technology-Aljufra-Sokna-Libya
^{2,3}Department of Chemical Engineering, University Malaysia Pahang- Malaysia

Abstract: The exists of hydrogen sulfide (H₂S) gas in gas treating plants increases the severity of corrosion due to the increased aggressiveness. The most commonly used material in the oil and gas industry is carbon steel, because of its low cost and abundant availability. In gas treating plants, amine solutions like monodiethanolamine (MDEA) are used for the removal of H₂S gas. However, hydrogen sulfide gas makes the monodiethanol amine (MDEA) solution corrosive. To study the corrosion behavior of carbon steel in (MDEA) solution, an electro- chemical DC corrosion testing technique has been used by exposing the carbon steel to 15% MDEA solution in the presence of hydrogen sulfide gas in various concentrations (blank solution, 2480,4840,7500 10,000) ppm. With an increase of hydrogen sulfide (H₂S) gas concentration, a very prominent shift in potentio dynamic plot was observed with an increase in corrosion rate from 0.1129 mpy form blank solution to 2.0675mpy for 10.000 ppm solution.

Keywords: Carbon Capture and Storage; absorbent, corrosion; MDEA/DC, Gas sweetening plant

Date of Submission: 02-12-2020

Date of Acceptance: 17-12-2020

I. INTRODUCTION

Corrosion is one of the great operational problems, faced by the gas plant and oil industry. Hydrogen sulfide (H₂S) creates sever corrosion for the equipment ,especially in gas plants, therefore the usage of Amine solutions in order to have low corrosion rate environment for economical transportation cost of gas refineries and utilities.

Sun and Nestic [2] studied the uniform H₂S corrosion of mild steel in order to predict the rate of corrosion over time at pH 5.0–5.5. They reported that the corrosion rate increased with an increase in H₂S gas concentration but the magnitude of the corrosion rate is lower after 24 hours compared to 1 hour because of the build-up of a protective iron sulfide film. Matsunami et al. [3] studied the effect of H₂S gas concentration at room temperature and reported an increase in corrosion rate with increasing gas concentration.

Amines are compounds that have a chemical structure derived from ammonia in which the hydrogen atoms are replaced by organic radicals [4]. These compounds are categorized in three types as shown in Table 1:

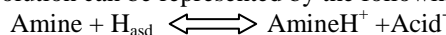
Table 1: Types of the compounds amines

Amine Type	Example	Chemical formula
First amines	Monoethanolamine (MEA)	CH ₂ CH ₂ OHNH ₂
Second amines	Diethanolamine (DEA)	(CH ₂ CH ₂ OH) ₂ NH
Third amines	Methyldiethanol amine (Mdea)	CH ₃ N(CH ₂ CH ₂ OH) ₂

Absorption by amines has been used since the early 1930s for the removal of hydrogen sulfide (H₂S) and/or carbon dioxide (CO₂) gas from natural gas in refineries and oil and gas fields [5–8]. The process is constantly subject to a number of operational difficulties, of which the most severe is corrosion.

II. CORROSION IN AMINE SOLUTIONS

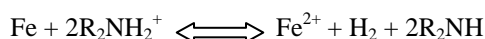
Corrosion in amine solutions is believed to be due to the reaction with absorbed acid gases (H₂S and/or CO₂) [4–10]. Amine solutions remove contaminants by acting as a base and taking a hydrogen ion from the acid that is formed by the dissociation of the gas in the water/amine solution. Labbe et al. [11] reported that acids react with amine by a proton transfer reaction due to the availability of a free electron pair on the nitrogen atom. Acid gas absorption by the amine solution can be represented by the following general reaction [6]:



For the H₂S loaded systems, Hacid is represented by H₂S and Acid⁻ by HS⁻. Amine H⁺ is a protonated amine ion, denoted “bound amine”, because it cannot react with any more acid gas. The simplified reactions for H₂S absorption by secondary amines (DEA) is shown below [4, 5, 12]:



The protonated amine ion (R_2NH_2^+) formed as a consequence of the absorption reaction causes dissolution of metal according to the reaction suggested by Kosseim et al. [13] as shown below:



The protonated amine ions are acids, in that they can provide protons for the corrosion reaction. The corroding metal reacts with the most abundant acid in the solution. In the case of amine solutions, protonated amine ions are much more concentrated than the hydrogen ions and, therefore, the mechanism of metal dissolution for amine solutions corrosion can be best represented by the reaction proposed by Kosseim et al. [13] shown above. The possible oxidizers for H_2S loaded amine system could be H_3O^+ , undissociated water (H_2O), and HS^- . These oxidizers cause the formation of corrosion products $\text{Fe}(\text{OH})_2$ and FeS , as shown by reactions in the above table. H_2S and H_2O play a dominant role governing the reduction reactions [14].

With the increase of acid gas (H_2S and/or CO_2) loading (concentration), the corrosivity of solution also increases. Acid gas loading for amine solutions is described as moles acid gas per mole amine. Amine solutions having higher hydrogen sulfide (H_2S) gas concentrations were found to be more corrosive than those amine solutions having low hydrogen sulfide (H_2S) gas concentration.

III. EXPERIMENTAL DETAILS

❖ Material under Investigation

The material used for this study is ASTM A-106 Grade-A carbon steel. The composition of material is shown in Table 2:

Table 2: The composition of material

Element	Mn	Si	C	S	P	Cr	Ni	Mo	V	Cu	Fe
Wt %	0.23-0.27	≤ 0.1	≤ 0.25	≤ 0.25	≤ 0.035	≤ 0.4	≤ 0.4	≤ 0.15	≤ 0.08	≤ 0.4	≤ Bal

Specimens were cut from a piece of used pipeline having dimensions of $10 \times 10 \times 5$ mm. These specimens were soldered to copper wire at the back and then cold mounted by using epoxy in silicon rubber moulds. The whole copper wire was then insulated in a glass tube. After mounting, these specimens were polished to 1000 grade SiCemery paper, in order to expose the surface to the electrolyte.

❖ Environment

The media employed in the electrochemical tests as electrolyte was 15% monodiethanolamine (MDEA) solution. This solution was used in the presence of hydrogen sulfide (H_2S) gas at varying concentrations, hydrogen sulfide gas in various concentrations (blank solution, 2480, 4840, 7500, and 10,000) ppm i. The concentration of H_2S in the solutions was determined by isometric titration as reported by Soosaiprakasam and Veawab [16]. Hydrogen sulfide gas was produced through Kipp's Apparatus using sulfuric acid and iron sulfide [17].

❖ Electrochemical Measurements

The electrochemical polarization techniques were performed to measure the corrosion rates and to study the corrosion behavior. Experiments were carried out using "DC 105 Corrosion measurement techniques", an application of the Gamry® Framework, and an electrochemical cell. A saturated calomel electrode (SCE) was used as a reference electrode and a platinum rod was used as a counter electrode. All the experiments were conducted at room temperature. Potentiodynamic polarization measurements were conducted to study the corrosion behavior from free corrosion potential (E_{corr}) to cathodic (-200 mV) and anodic (1500 mV) potentials versus open circuit potential at a scan rate of 20 mV/sec.

For corrosion rate measurements, Tafel plots were generated by polarizing the specimen about 250 mV anodically and cathodically from E_{corr} . The resulting current is plotted on a logarithmic scale against potential. The corrosion current density (i_{corr}) was obtained from Tafel plot by extrapolating the linear portion of the curve to E_{corr} ; this extrapolating facility was available with the software used, i.e., the dedicated software of Gamry® framework.

The corrosion rate was calculated from the i_{corr} using the following relation [18]:

$$\text{Corrosion Rate} = K M i_{\text{corr}} / nD$$

Where:

M = atomic weight of metal,

i_{corr} = current density in $\mu\text{A}/\text{cm}^2$,

n = number of electrons transferred (valence change),

D = density in g/cm^3 , and

K = a constant depending on the penetration rate desired; for mpy (millinch or mils per year), $\mu\text{m}/\text{yr}$, and

mm/yr the values of K are 0.00286, 0.0115055, 0.0235781, and 0.0525169 respectively.

IV. RESULT AND DISCUSSION

❖ Potentiodynamic Curves and Tafel Plots in 15% MDEA Solution

Fig 1 shows the potentiodynamic curves for the lank Solution obtained by exposure of ASTM A-106 Grade A carbon steel in 15% MDEA solution in the presence of hydrogen sulfide gas at different concentrations.

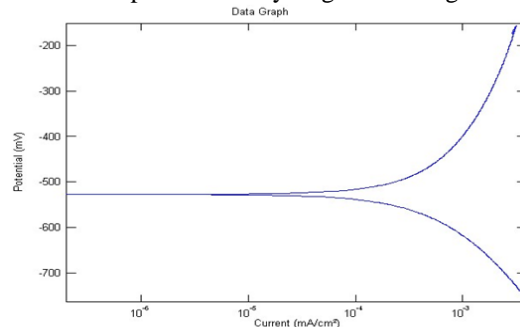


Fig 1: The potentiodynamic curves for the lank Solution

Curve A represents the potentiodynamic curve obtained in 15% MDEA solution which was not saturated with H_2S gas (i.e., $H_2S \approx 0$ ppm). In this case, a very sharp change from active to passive behavior is observed at low current values, suggesting that environment is favorable for formation of a stable protective film (possibly iron sulfide or ferrous hydroxide). With the increase of potential, passivity, which may be due to the presence of oxygen in the environment, breaks down at about 600 mV. However, a low corrosion rate (0.00286 mpy; as calculated using Equation 5) was observed before passivity breakdown, as estimated from Tafel plot (Fig 2 (a)).

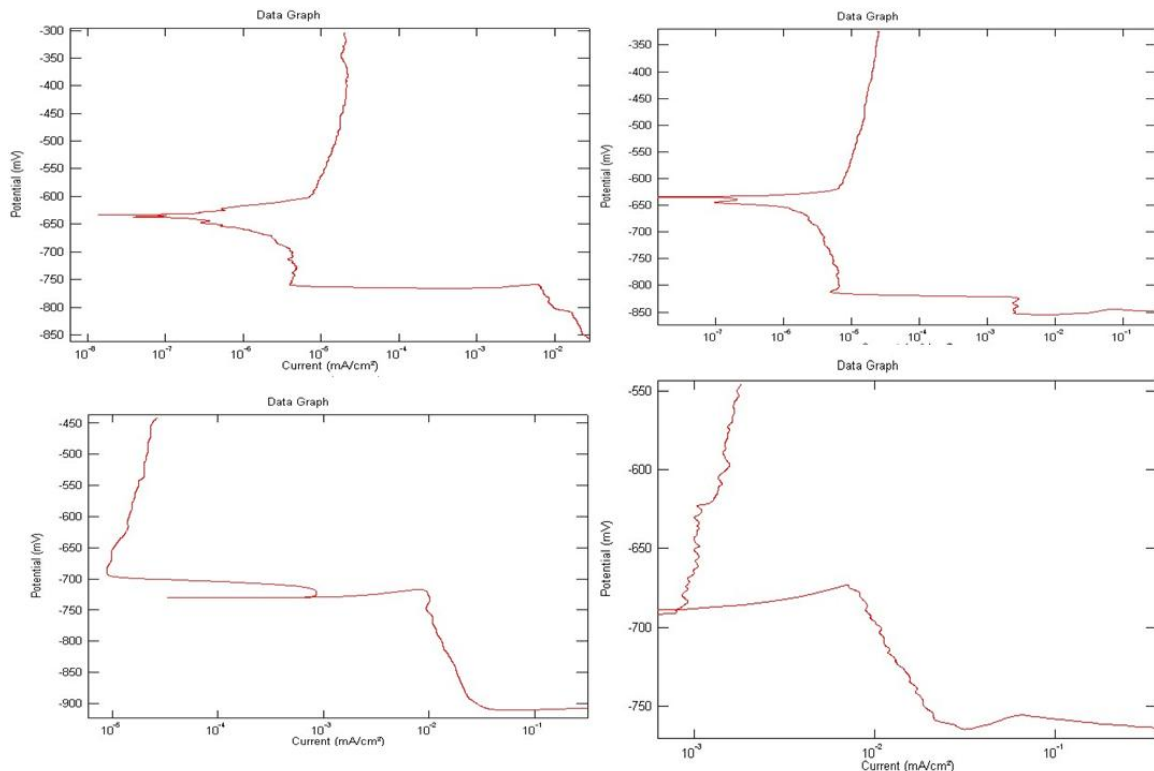


Fig 2 : Tafel plots in 15 % MDEA solution at different H_2S concentrations

Curve B (Fig 1) represents the potentiodynamic curve obtained in 15% MDEA solution saturated with H_2S gas (i.e., $H_2S \approx 2840$ ppm). In this case, the anodic reaction accelerates as noted from the active shift of the corrosion potential to about -700 mV due to the presence of H_2S gas in the environment. Hydrogen sulfide gas dissociates into aggressive species (HS^- , H^+ , and S^{2-}) as it comes in contact with water in amine solution, which causes an increase in the anodic current density and, hence, a high corrosion rate is observed. The corrosion rate obtained from Tafel plot (Fig 2 b) is 0.0115055mpy (as calculated using Equation 5). Another

reason for the increase in corrosion rate is the formation of protonated amine ions ($R_2NH_2^+$). Anodic noses appear in the curves as exhibited in Fig 1 (curves B, C, and D), due to subsequent formation and breakage of corrosion product film. These anodic noses suggest that MDEA does not form a good protective film in the presence of hydrogen sulfide gas. The reason for the breakage of the film may be the volume of the film. It is reported [2] that the film formed on exposed surface is more voluminous than the iron it replaces, which creates stresses that result in damage of the film.

In order to study the effect of concentration of H₂S gas on corrosion behavior in 15% MDEA solution, the concentration of hydrogen sulfide gas was increased and the 15% MDEA solution was saturated with H₂S gas up to approximately 7500 ppm and a potentiodynamic curve was obtained as shown by curve C (Fig 1). With the increase of H₂S gas concentration, the curve shifts to more positive values (as revealed by curve D) and anodic current density increases to higher values because of the increase of aggressiveness of environment with the increase of aggressive species (HS⁻, H⁺, and S₂⁻) and, hence, corrosion rate increases. Another reason for the increase in corrosion rate is the formation of more protonated amine ions ($R_2NH_2^+$). The greater the concentration of protonated amine ions, the greater will be the dissolution of iron. The corrosion rate obtained from Tafel plot at approximately 7500 ppm H₂S gas (Figur 2 c) is 0.0235781mpy. Again, an anodic nose appears in the potentiodynamic curve, which represents subsequent formation and breakage of corrosion product film.

Curve D (Fig 1) represents the potentiodynamic curve obtained in 15% MDEA solution saturated with higher H₂S gas concentration (H₂S ≈ 10000 ppm). In this case, the anodic current density increases to higher values and, hence, a high corrosion rate is observed. The corrosion rate obtained from Tafel plot (Fig 2 d) is 0.0525169 mpy, which is higher than previous cases. Due to higher H₂S concentration, the amount of protonated amine ions will be increased, which may be another reason of increased corrosion rate at higher H₂S concentration compared to that at low concentration. An anodic nose is also present, Fig 1D, but not very sharp, which suggests that MDEA is not a good film forming a mine in the presence of hydrogen sulfide gas.

From Fig 1, it is obvious that with the increase of H₂S concentration, the potentiodynamic curve shifts to higher values and anodic current density increases to higher current values due to which corrosion rate increases with increase of H₂S concentration. Also, the region of passivity due to film formation is decreased with increase of H₂S gas concentration, and at 10000ppm H₂S gas, this region was very minute in the potentiodynamic curve.

Table 3: A-Data Obtained From the Laboratory Experiment for 2480 PPM of H₂S Solution

Test type	Instrument serial number	Physical channel	Sequence number	ZRA Number	Time and Date	Data points	Area (cm ²)
Cyclic sweep	1543	1	1	n/A	14/4/2012	1819	1
Rest Potential (mV)	Metal	Metal factor	LPR (Ohm.cm ²)	Ba (mV)	Bc (mV)	I _{corr} (mA/cm ²)	Corrosion Rate (mm/year)
-599.14	Mild steel	1159	49541	120	120	0.0005266	0.0061029
Corrosion rate (mils/yr)	Intercept (mA/cm ²)	Intercept corrosion rate (mm/year)	Intercept corrosion rate (mils/yr)	IR Compensation value (Ohm.cm ²)	Start Potential	Reverse Potential	Sweep Rate
0.2402727	0	0	0	N/A	-300mV	300mV	20mV/min
Cycles	Readings Per Test	Gradual Sweep From Cell to Start Potential	Cell Settle Time	Count Resistor At Start	Count Resistor During Test	Offset To Rest Potential	Current Limit
1	Automatic	No	15 sec	auto	auto	yes	off

Time (Sec)	Potential (mV)	Current (mA/cm ²)
0	-848.6	-0.3183
56.624	-854.89	-0.00743
107.68	-841.89	-0.00266
158.31	-825.59	-0.00287
211.07	-817.11	-1.85E-05
259.32	-801.7	-6.65E-06
307.51	-786.8	-6.47E-06
356.13	-770.94	-6.29E-06
403.98	-754.97	-5.42E-06
452.31	-739.33	-4.89E-06
500.62	-723.7	-4.01E-06
548.68	-708.67	-3.93E-06

596.93	-693.47	-3.32E-06
645.82	-678.2	-2.35E-06
694.07	-663.16	-1.78E-06
743.51	-647.73	-2.18E-07
801.71	-629.86	1.13E-06
856.46	-612.65	6.94E-06
911.09	-595.62	8.13E-06
965.78	-578.87	9.32E-06
1019.9	-562.62	1.01E-05
1069.2	-547.39	1.09E-05
1118.5	-532.29	1.20E-05
1166.9	-517.51	1.28E-05
1215.5	-504.39	1.42E-05
1263.6	-489.84	1.53E-05
1312.2	-474.35	1.57E-05
1361	-459.01	1.63E-05
1409	-443.97	1.72E-05
1457.1	-428.71	1.79E-05
1505.3	-415.55	1.97E-05
1553.6	-400.82	2.05E-05
1602.4	385.91	2.14E-05
1650.5	-371.19	2.25E-05
1698.7	-356.59	2.30E-05
1746.8	-342.11	2.41E-05
1795.1	-327.78	2.55E-05
1804.5	-327.49	2.49E-05

V. CONCLUSION

1. Corrosion rates are increased by high amine concentration, high acid gas loading, high temperatures, degradation products, and foaming. Also corrosive acid gases flashed from solution, anodic current density increases very rapidly and corrosion current density shifted towards higher values.
2. MDEA products have improved performance in many amine systems.
3. Amine solutions are non-corrosive but the presence of H₂S gas makes these solutions corrosive.

REFERENCES

- [1]. J. Szyprowski, "Methods of Investigation on Hydrogen Sulfide Corrosion of Steel and Its Inhibitors", Corrosion (NACE), 59(1)(2003), pp. 68–81.
- [2]. W. Sun and S. Nestic, "A Mechanistic Model of H₂S Corrosion of Mild Steel", Corrosion (NACE), (2007), Paper No. 07655.
- [3]. K. Matsunami, T. Kato and K. Sugimoto, "Corrosion of Carbon Steel and Its Estimation in Aqueous Solution Used in Petroleum Refineries", Int. Journal of Pressure Vessel and Piping, 45(1991), pp. 179–197.
- [4]. S. Rennie, "Corrosion and Materials Selection for Amine Service", Materials Forum, 30(2006), pp. 126–130.
- [5]. R. R. Veldman, "Alkanolamine Solution Corrosion Mechanisms and Inhibition from Heat Stable Salts and CO₂", Corrosion (NACE), (2000), Paper No. 00496.
- [6]. E. Keller, A. L. Cummings and F. C. Veatch, "Corrosion and Corrosion Control Methods in Amine Systems Containing H₂S", Corrosion (NACE), (1997), Paper No. 341.
- [7]. J. J. Gonzalez, S. Hernandez, and A. Vilorio, "Stress Corrosion Cracking of Carbon Steels in Amine Units", Corrosion (NACE), (1998), Paper No. 405.
- [8]. D. Fan, L. E. Kolp, D. S. Huett, and M. A. Sargent, "Role of Impurities and H₂S in Refinery Lean DEA System Corrosion", Corrosion (NACE), (2000), Paper No. 00495.
- [9]. H. L. Craig and B. D. McLaughlin, "Corrosive Amine Characterization", Corrosion, (1996), Paper No. 394.
- [10]. M. J. Litschewski, "More Experiences with Corrosion and Fouling in a Refinery Amine System", Corrosion (NACE),(1996), Paper No. 391.
- [11]. J. C. Labbe, J. Mexmain, and A. A. Khan, "Chemistry of Aqueous Solutions Electrochemistry", Alhamra Publishing, 2004.
- [12]. M. Nouri and D. R. Clarida, "Interaction of Process Design, Operating Conditions and Corrosion in Amine Systems", Corrosion (NACE), (2007), Paper No. 07398.
- [13]. J. Kosseim, J. G. McCullough, and K. F. Butwell, "Corrosion-Inhibited Amine Guard ST Process", Chemical Engineering Progress, 80(10)(1984), pp. 64–71.
- [14]. A. Veawab and A. Aroonwilas, "Identification of Oxidizing Agents in Aqueous Amine–CO₂ Systems Using a Mechanistic Corrosion Model", Corrosion Science, 44(2002), pp. 967–987.
- [15]. A. Barreau, E. Blanchon le Bouhelec, K. N. H. Tounsi, P. Mougain, and F. Lecomte, "Absorption of H₂S and CO₂ in Alkanolamine Aqueous Solution: Experimental Data and Modelling With the Electrolyte-NRTL Model", Oil & Gas Science and Technology – Rev. IFP, 61(3)(2006), pp. 345–361.
- [16]. R. Soosaiprakasham and A. Veawab, "Corrosion and Polarization Behavior of Carbon Steel in MEA-Based CO₂ Capture Process", Int. J. Greenhouse Gas Control, doi:10.1016/j.ijggc.(2008), 02.009.
- [17]. M. Rabinowitch, Andrew Dingwall, and F. H. Mackay, 'Studies on Cerebrospinal Fluid', The Journal of Biological Chemistry, (1933), pp. 707-723.
- [18]. M. G. Fontana, Corrosion Engineering. Third Edition, McGraw Hill Publications, (1988).
- [19]. Gas/Spectechnolgy Group, M.S. Dupart ,T.R Bacon and D.J. Edwards , "UnderStanding Corrsion Alkanolamine Gas Treting Plants", (1993).<http://www.gastreating.com/pdf/hc%20processing%20apr-may%2019, 93.pdf>